REVIEW

Imaging Morphogenesis: Technological Advances and Biological Insights

Philipp J. Keller

Morphogenesis, the development of the shape of an organism, is a dynamic process on a multitude of scales, from fast subcellular rearrangements and cell movements to slow structural changes at the whole-organism level. Live-imaging approaches based on light microscopy reveal the intricate dynamics of this process and are thus indispensable for investigating the underlying mechanisms. This Review discusses emerging imaging techniques that can record morphogenesis at temporal scales from seconds to days and at spatial scales from hundreds of nanometers to several millimeters. To unlock their full potential, these methods need to be matched with new computational approaches and physical models that help convert highly complex image data sets into biological insights.

Vertebrates and higher invertebrates start as a single cell that develops into a fully functional organism comprising tens of thousands to trillions of cells, which are arranged in tissues and organs able to perform highly complex tasks. Understanding development as a function of cell behavior at this system-wide level is a central goal of biology. This investigation, however, faces fundamental challenges, because morphogenesis—i.e., the shaping of an organism by cell movements, cell-cell interactions, collective cell behavior, cell shape changes, cell divisions, and cell death—is a dynamic process on multiple spatial and temporal scales: from submicrometer and subsecond dynamics of macromolecules inside each cell, to changes of cell shape that occur on the scale of micrometers within seconds, to cell movements that take place over distances of tens to hundreds of micrometers within minutes to hours, to structural changes on the tissue- and whole-organism level encompassing millimeter to centimeter length scales and hours to days of development (Fig. 1). Thus, the ability to capture, simultaneously, the fast dynamic behavior of individual cells, as well as their system-level interactions over long periods of time, is crucial for an understanding of the underlying biological mechanisms.

Howard Hughes Medical Institute, Janelia Farm Research Campus, 19700 Helix Drive, Ashburn, VA 20147, USA.
E-mail: kellerp@janelia.hhmi.org

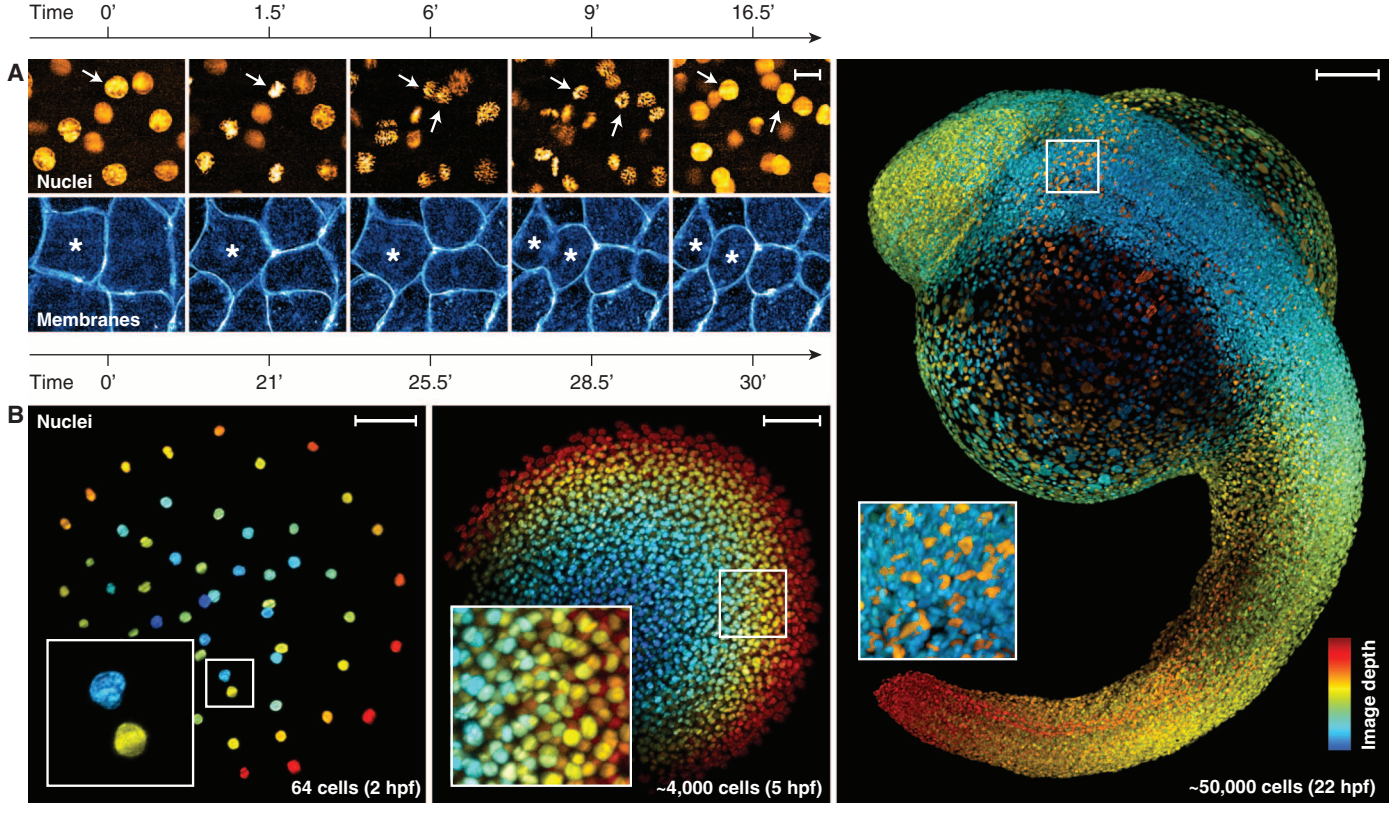

Fig. 1. Spatiotemporal scales of morphogenesis. Morphogenesis, illustrated here for the zebrafish embryo, involves multiple spatial and temporal scales: from fast, local cell shape changes and cell movements (A) to slow but large-scale structural changes on the tissue- and whole-embryo level (B). Images were recorded with digital scanned laser light-sheet microscopy (DSLM) and simultaneous multiview light-sheet microscopy (SiMView) (*2*, *25*). (**A**) Nuclei (top) and membrane (bottom) dynamics in two different locations of a 2-hour-old zebrafish embryo. Arrows and asterisks highlight examples of dividing cells. (**B**) Whole-embryo projections of nuclei-labeled zebrafish embryos at different developmental stages, showing the rapid increase in cell count and morphological complexity in early embryogenesis. Insets: enlarged views of highlighted areas. Scale bars: 20 μm (A), 100 μm (B).

In addition to tackling the spatial and temporal challenges associated with the observation of single-cell to tissue-level morphological dynamics (*1*–*3*), a comprehensive understanding of morphogenesis requires quantitative measurements of protein dynamics (*4*), changes in gene expression (*5*–*7*), and (direct or indirect) readouts of physical forces acting during development (*8*). Knowing the spatiotemporal relationship of these core constituents is often the key to elucidating developmental mechanisms. Live-imaging approaches based on light microscopy are of central importance to obtain such information at the system level and with high spatiotemporal resolution (Fig. 2).

The development of advanced microscopy technology for noninvasive in vivo imaging is indispensable for advancing our understanding of morphogenesis. It is now feasible to obtain comprehensive information on the cellular dynamics in entire developing vertebrate and higher invertebrate embryos throughout their development (movies S1 to S10). It is possible to record cell movements, cell shape dynamics, cell divisions, and gene expression information simultaneously, for the entire undisturbed living system. At the same time, substantial efforts are underway to experimentally characterize the biophysical properties of tissues, in particular the parameters describing their responses to external mechanical forces and the adhesive behavior of their cellular components (*9*).

With the emergence of powerful, new imaging techniques that produce large image data sets of complex developmental processes at unprecedented detail, it is equally important to devise new computational methods to analyze such microscopy data in a biologically meaningful way. By integrating biological material properties with comprehensive live-imaging data of entire developing embryos at the subcellular level, computational models of morphogenesis with predictive power—projecting the tissue- or even embryo-wide morphogenetic consequences of genetic or mechanical perturbations—are finally within reach.

Challenges in the Live Imaging of Morphogenesis

Live-imaging applications require carefully balancing competing parameters (Fig. 3). High imaging speeds are required to capture fast cellular processes and to facilitate effective live imaging of large biological specimens. High spatial resolution is needed to follow intracellular processes or to resolve structural details of cell-cell interactions. High signal-to-noise ratios are crucial to obtain interpretable images and to robustly automate computational image analysis. Long observation periods are needed to capture continuous data sets of nonstereotypic processes over relevant developmental time scales. Comprehensive physical coverage is required to follow developmental events on the whole-organism level. Finally, low levels of light exposure are essential to reduce photobleaching of fluorescent markers and minimize phototoxic effects that may impact normal development.

These key parameters are limited by fundamental physical and biological constraints that are independent of microscope design. For example, with a given amount of fluorescent proteins, spatial resolution can be improved only at the expense of temporal sampling, signal-to-noise ratio, or maximum observation length, owing to the higher light exposure of the sample and increased rate of fluorescent protein consumption (Fig. 3A). The optimal imaging method thus makes maximum use of the parameter space that is allowed. The requirement of practical applicability to live observations of biological processes

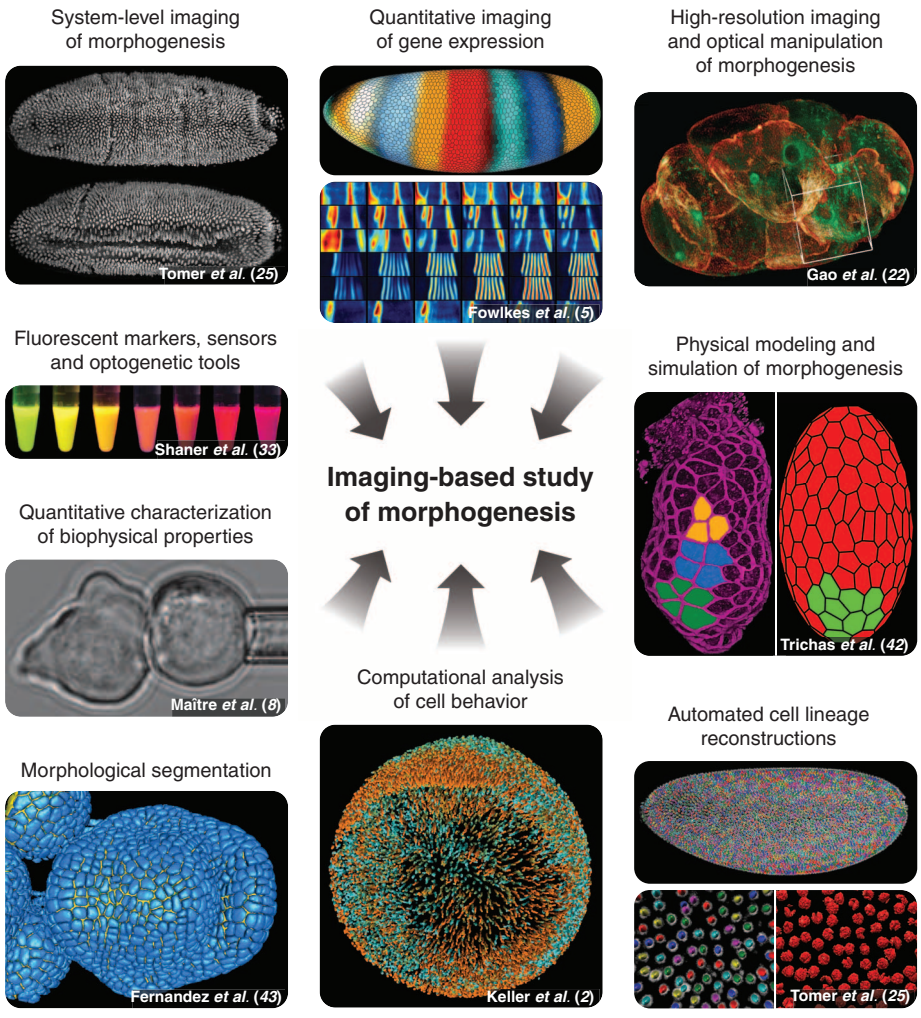

Fig. 2. Imaging-based study of morphogenesis. The imaging-based study of morphogenesis involves optical methods, biotechnology, and biophysical measurements, as well as physical modeling and computational approaches to image analysis. Specific examples of these general classes of techniques are depicted in each box. Often, most—if not all—of these approaches are combined to arrive at a quantitative understanding of morphogenetic processes. Clockwise, from top right panel: High-resolution Bessel SR-SIM live imaging of myosin (green) and membranes (orange) in an early *C. elegans* embryo [reprinted from (*22*)]; imaging (left, examples of groups of cells that share a central vertex highlighted in color) and modeling (right, anterior visceral endoderm cells shown in green) of an early mouse embryo [reprinted from (*42*)]; automated cell lineage reconstruction in the *Drosophila* syncytial blastoderm (top: whole embryo, bottom: enlarged view) [reprinted from (*25*)]; global cell tracking in the early zebrafish embryo [reprinted from (*2*)]; cell segmentation in an *Arabidopsis* flower [reprinted from (*43*)]; assay for measuring mechanical parameters controlling cell-cell contact formation by ex vivo adhesion of progenitor cell doublets [reprinted from (*8*)]; fluorescence image of purified proteins mHoneydew, mBanana, mOrange, tdTomato, mTangerine, mStrawberry, and mCherry (from left to right) [reprinted from (*33*)]; SiMView live imaging of a nuclei-labeled *Drosophila* embryo at the onset of gastrulation (top: dorsal view, bottom: ventral view) [reprinted from (*25*)]; visualization of gene expression data obtained by two-photon imaging of early *Drosophila* embryos (top: expression of gap genes *fkh*, *gt*, *hb*, *kni*, and *Kr*; bottom: expression of *kni*, *gt*, *hb*, *eve*, *ftz*, and *slp1* at different time points) [reprinted from (*5*)].

(Figs. 3B and 4 and movies S11 to S15) often favors an overall optimization of performance over a microscope design that provides a substantial improvement in a single parameter at the expense of others. Although different live-imaging techniques are qualitatively constrained by the same fundamental trade-offs, they often exhibit substantial performance differences as the direct result of their methodological design.

Confocal fluorescence microscopes are currently the most commonly used imaging systems with optical sectioning capability [the ability to resolve three-dimensional (3D) structures]. This mature, commercially available technology represents a state-of-the-art approach to studying morphogenesis by live imaging and can resolve biological processes on a multitude of spatial scales, from subcellular to whole-tissue level (Fig. 4, B to D, and movies S7, S9, S11 to S13, and S15).

In point-scanning confocal fluorescence microscopy, a beam of laser light is focused into the specimen to excite fluorescent molecules. Fluorescence light is generated especially, but not exclusively, at the focus. To ensure that only fluorescence light originating from the small focal volume is detected, a small pinhole in the detection system is used to block out-of-focus signal. An entire 3D image can thus be recorded by scanning the laser focus through the sample and measuring the signal sequentially at each focus position.

A major drawback of this concept is the very inefficient use of light and fluorescent markers, as well as the very high light exposure of the sample. At the same time, the point-scanning approach introduces a fundamental imaging speed limit. The discovery of two-photon excitation presents an effective approach to address the first issue: Laser light at approximately twice the conventional wavelength is used to excite fluorescence only in the focal volume, where the power density is high enough to efficiently trigger multiphoton absorption. The use of this longer-wavelength light also allows penetrating deeper into biological tissues (*10*) (Figs. 4A and 5, A and B, and movies S1 and S14). However, in the conventional implementation of this approach as a point-scanning technique, it suffers from the same limitations in speed and signal-to-noise ratio as confocal fluorescence microscopy.

To address these limitations, a new fluorescence imaging method was developed that combines intrinsic optical sectioning with wide-field detection. This method, known as light-sheet microscopy (*11*, *12*), allows entire multimegapixel images to be acquired in a single, spatially confined illumination step: In contrast to the point excitation approach in confocal microscopy, an entire micrometer-thin volume is illuminated with laser light entering the sample from the side. The fluorescence emitted by reporter molecules in this thin volume is collected with an objective lens oriented at a right angle to the light sheet.

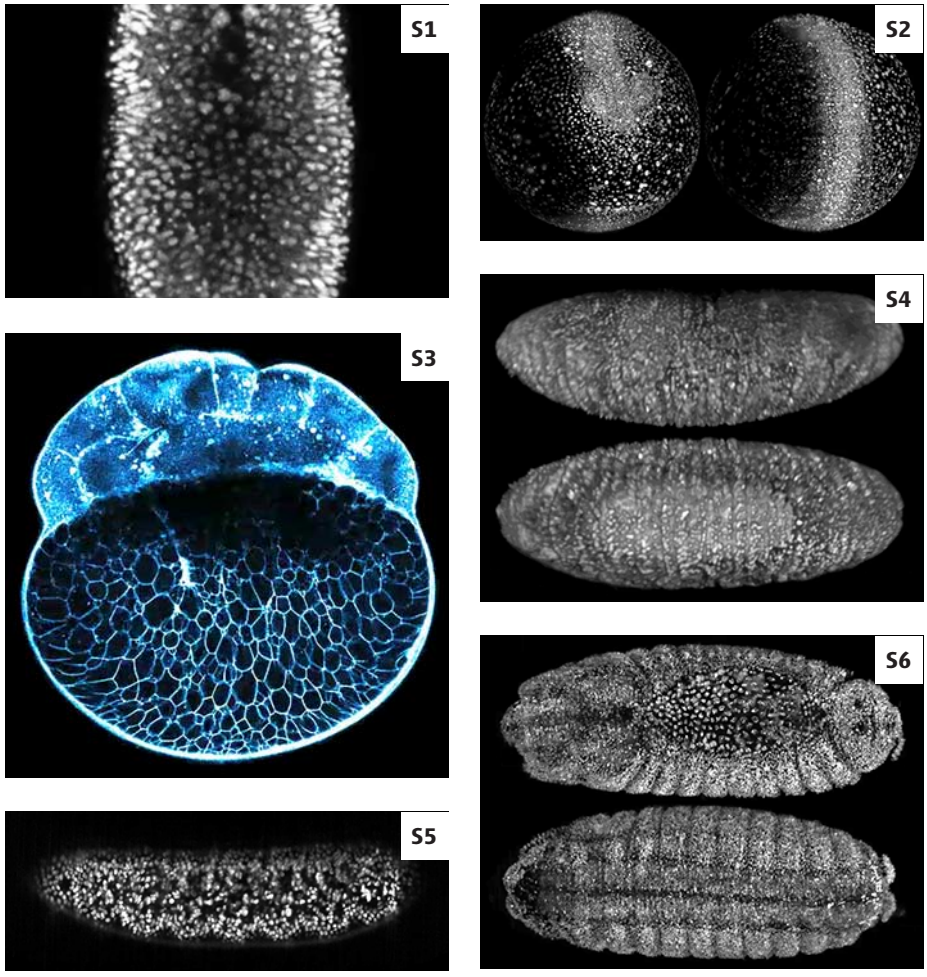

Movie S1. Imaging mesoderm spreading in the *Drosophila* embryo with point-scanning two-photon microscopy. Dorsal (part 1) and posterior (part 2) views of a H2A-GFP expressing embryo are shown. This movie was published previously (*1*). [Credit: McMahon *et al*. 2008 (*1*)]

Movie S2. Multiview imaging of zebrafish embryonic development with digital scanned laser light-sheet microscopy (DSLM). The H2B-eGFP mRNA injected zebrafish embryo was imaged from the 64-cell stage for 25 hours in intervals of 90 s (453,620 high-resolution images, 3.5 TB). This movie was published previously (*2*). [Credit: Keller *et al*. 2008 (*2*)]

Movie S3. Third-harmonic generation (THG) imaging of the early zebrafish embryo. THG imaging (1200 nm excitation wavelength) started in the one-cell stage. A sagittal thick slice is displayed. Scale bar: 100 μm. This movie was published previously (*50*). [Credit: Olivier *et al*. 2010 (*50*)]

Movie S4. Imaging *Drosophila* embryogenesis with two-photon light-sheet microscopy (2p-SPIM). 3D-rendered views of a fly embryo with GFP-labeled nuclei are shown over a period of 18 hours. Scale bar: 100 μm. This movie was published previously (*24*). [Credit: Truong *et al*. 2011 (*24*)]

Movie S5. Imaging a stage 16 *Drosophila* embryo with simultaneous multiview two-photon light-sheet microscopy (2p-SiMView). The volume of a nuclei-labeled *Drosophila* embryo is shown slice by slice. This movie was published previously (*25*). [Credit: Tomer *et al*. 2012 (*25*)]

Movie S6. Imaging *Drosophila* embryogenesis with simultaneous multiview light-sheet microscopy (SiMView). The fly embryo with GFP-labeled nuclei was imaged for 17 hours in intervals of 30 s (1,066,520 high-resolution images, 11 TB). This movie was published previously (*25*). [Credit: Tomer *et al*. 2012 (*25*)]

Although this approach is derived from a more than 100-year-old idea (*13*), its outstanding practical performance has been demonstrated only recently (*12*). Light-sheet fluorescence microscopy provides substantially improved imaging speed and signal-to-noise ratio, while minimizing the light exposure of the specimen (*14*) (Figs. 1 and 5, C to F, and movies S2, S4 to S6, S8, and S10). It is thus particularly well suited to biological live-imaging applications (*15*) and has an

outstanding potential in the systematic, quantitative study of development (*2*, *12*) and function (*16*, *17*) of complex biological systems.

Novel Approaches and Recent Advances in Light Microscopy

Confocal and two-photon fluorescence imaging approaches have gone through numerous iterations of refinement and optimization over the course of several decades. Powerful commercial systems are readily available, and recent conceptual advances in light microscopy may soon open the door to an entirely new generation of these methods (*18*–*20*). By contrast, the emerging field of light-sheet microscopy still largely relies on custom-built instruments, some of which have been crafted as highly affordable hybrids by extending basic commercial imaging platforms with custom light-sheet illumination modules (*3*). In the past 2 years, the development of light-sheet–based fluorescence microscopy has experienced rapid progress, which is of particular relevance to the imaging-based study of morphogenesis. These advances address the most critical limitations of conventional techniques; namely, spatial resolution (*21*, *22*) (Fig. 5D and movie S10), imaging speed (*3*, *16*, *23*) (Fig. 5C and movies S7 and S8), and optical access to developmental processes in nontransparent living organisms (*24*–*26*) (Fig. 5, E and F, and movies S4 to S6). By virtue of these new capabilities, state-of-the-art light-sheet microscopes enable the design of live-imaging experiments that were previously not possible.

Spatial Resolution

Bessel beam light-sheet microscopy provides substantially improved spatial resolution (*21*). In conventional scanned light-sheet microscopy, a thin volume section of the sample is illuminated by rapidly moving a weakly focused Gaussian laser beam across the field-of-view (*2*). Because the laser beam is oriented parallel to the recorded plane, its thickness directly influences the axial resolution of the microscope, which is typically on the order of a few micrometers. By using Bessel beams with a thinner central intensity peak for specimen illumination, the axial resolution can be substantially improved, to the point where it becomes comparable to the typically much better lateral resolution—on the order of 300 nm—of the microscope (*21*). In addition, the use of Bessel beams has been shown to reduce the overall amount of scattering-induced image artifacts and improve penetration of biological tissues (*27*).

The Bessel beam's thin core is surrounded by a series of concentric rings, which, if left unaccounted for, will degrade image quality compared to a recording made with Gaussian beams. However, this issue can be mitigated, for example, by using structured illumination (i.e., patterned light for specimen illumination) (*28*, *29*) or two-photon excitation (*21*). Structured illumina-

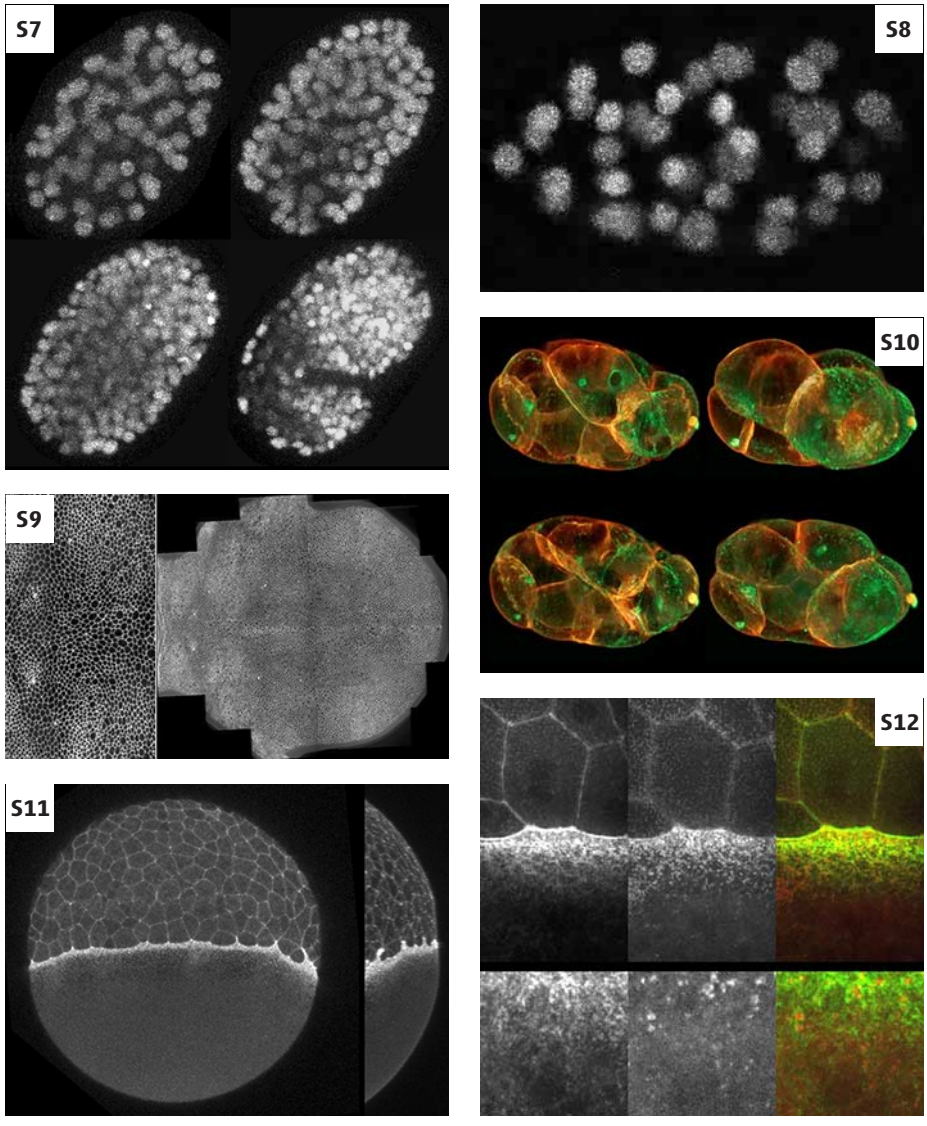

Movie S7. Imaging *C. elegans* embryogenesis with spinning-disk confocal microscopy. An embryo of the BV24 GFP-histone strain was imaged at 1 volume/min. This movie was published previously (*3*). [Credit: Wu *et al*. 2011 (*3*)]

Movie S8. Imaging *C. elegans* embryogenesis with inverted selective plane illumination microscopy (iSPIM). An embryo of the BV24 GFP-histone strain was imaged at 30 volumes/min from the two-cell stage until hatching. This movie was published previously (*3*). [Credit: Wu *et al*. 2011 (*3*)]

Movie S9. Imaging epithelium morphogenesis in the *Drosophila* dorsal thorax with spinning disk confocal microscopy. Dorsal thorax tissue expressing E-Cad:GFP was imaged between 11 and 35 hAPF in 5 min intervals. The positions of macrochaetae and midline are indicated by white circles and by a black dotted line, respectively. This movie was published previously (*36*). [Credit: Bosveld *et al*. 2012 (*36*)]

Movie S10. Imaging early *C. elegans* embryogenesis with Bessel beam super-resolution structured plane illumination microscopy (SR-SIM). Membrane dynamics during early embryonic development (part 1) and relationship between membrane morphology and myosin expression (part 2) are shown. This movie was published previously (*22*). [Credit: Gao *et al*. 2012 (*22*)]

Movie S11. Imaging zebrafish epiboly with confocal fluorescence microscopy. *Tg(actb1:GFP-utrCH)* labeling F-Actin was imaged throughout the course of epiboly (40-90% epiboly). Left: Lateral view. Right: Orthogonal view. Scale bar: 100 μm. This movie was published previously (*37*). [Credit: Behrndt *et al*. 2012 (*37*)]

Movie S12. Imaging actomyosin flows in zebrafish epiboly with spinning-disk confocal fluorescence microscopy. *Tg(actb1:myl12.1-eGFP)* labeling Myosin-2 (left), injected with lifeact-RFP mRNA labeling F-Actin (middle), was imaged at 60 to 70% epiboly. Right: Dual-color merge. White rectangle indicates region of magnified view (bottom). Scale bars: 10 μm. This movie was published previously (*37*). [Credit: Behrndt *et al*. 2012 (*37*)]

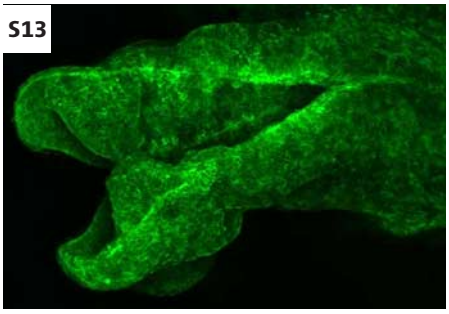

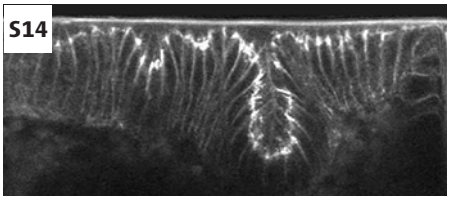

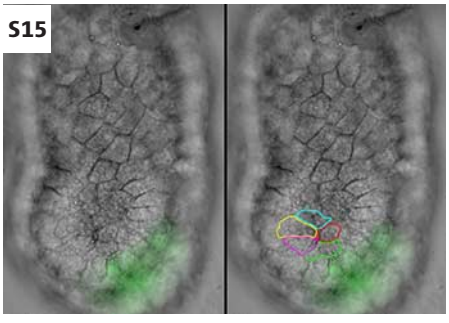

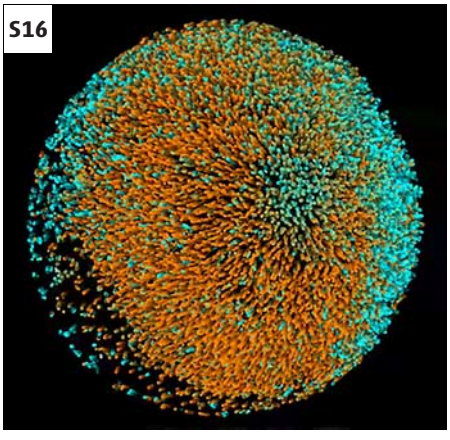

Movie S13. Imaging neural tube closure in the mouse embryo with confocal fluorescence microscopy. Movie shows dorsal side of a 13-somite wild-type embryo expressing Ven^{Myr} highlighting cell membranes. Scale bar: 100 μm. This movie was published previously (*51*). [Credit: Massarwa and Niswander 2013 (*51*)]

Movie S14. Imaging the dynamics of adherens junctions during *Drosophila* dorsal fold formation with point-scanning two-photon microscopy. An optical mid-sagittal section of the dorsal epithelium expressing E-Cadherin-GFP was imaged every 5 s from late cellularization to early gastrulation. This movie was published previously (*39*). [Credit: Wang *et al*. 2012 (*39*)]

Movie S15. Imaging mouse development with confocal fluorescence microscopy. Time-lapse movie shows rosettes forming in the visceral endoderm during anterior visceral endoderm (AVE) migration. AVE cells are marked by Hex-GFP fluorescence (green). DIC images were acquired with the confocal's transmitted light PMT. Scale bar: 50 μm. This movie was published previously (*42*). [Credit: Trichas *et al*. 2012 (*42*)]

Movie S16. Reconstructing zebrafish embryonic development from DSLM image data. Orthographic rendering of the computational reconstruction of the data set shown in movie S2. Color-code indicates movement speed of each nucleus (cyan to orange: 0 to 1.2 μm/min). This movie was published previously (*2*). [Credit: Keller *et al*. 2008 (*2*)]

tion in scanned light-sheet microscopy has been shown to enable contrast enhancement in nontransparent living specimens (*30*), where image quality usually suffers from light scattering. By combining Bessel beam light-sheet microscopy with this type of illumination strategy, exceptionally high spatial resolution, image contrast, and signal strength can be achieved through subsequent image reconstruction with algorithms previously developed for superresolution structured illumination microscopy (SR-SIM) (*22*). In contrast to typical superresolution approaches, this method minimizes the energy load on the specimen, provides acquisition rates of hundreds of images per second, and is applicable to living multicellular specimens. Recently, this method has been used to image cell shape dynamics in entire developing *Caenorhabditis elegans* embryos at 200-nm lateral resolution and 400-nm axial resolution (*22*), demonstrating its potential for the study of morphogenesis (Fig. 5D and movie S10, study "h" in Fig. 3B).

Penetration Depth

Another key challenge in all light-based imaging techniques is the fundamentally limited penetration depth of light in biological tissues, which constrains imaging of large living specimens. Even in relatively transparent tissues, conventional methods generally only reach depths of several tens to a few hundreds of micrometers when using visible light. Strategies being developed to address this limitation include the use of adaptive optics (*18*, *31*) and deep-tissue penetration by acousto-optic fluorescence imaging (*19*, *32*). For example, through use of an approach to adaptive optics in which the rear pupil of the objective lens is segmented, substantial improvements in resolution and signal strength have been achieved at depths up to 400 μm into mammalian tissue, thereby addressing typical limitations in penetration depth arising from optical aberrations (*18*). Moreover, fluorescence imaging up to 2 mm deep inside highly scattering media has recently been demonstrated by modulating light propagation through the tissue with ultrasound pulses (*19*).

Penetration depth can also be increased by the use of fluorescent probes excitable with light of longer wavelengths (*33*, *34*), in particular in the far red or even infrared, where biological tissues generally scatter and absorb considerably less light and thus appear more transparent. The concept of nonlinear excitation in two-photon microscopy takes this idea one step further and constitutes a powerful and well-established strategy to facilitate observations inside living specimens at greater depths than are possible with conventional imaging approaches (Fig. 5, A and B, and movies S1 and S14). The recent introduction of nonlinear excitation in scanned light-sheet microscopy combines the strengths of both methods, enabling, for example, a twofold increase in penetration depth in live imaging of *Drosophila* embryos (*24*) (Fig. 5E and movie S4).

Imaging Speed and Spatial Coverage

By simultaneously recording multiple complementary views of the sample in a light-sheet microscope, fast cellular dynamics can be rapidly imaged even for large, nontransparent biological specimens (*25*, *26*) (Fig. 5F). This approach synergizes with the use of nonlinear excitation (movie S5) and enables quantitative analyses of biological processes at the system level, such as comprehensive cell tracking through the cell division waves in the blastoderm-stage *Drosophila* embryo (*25*). In addition, light-sheet–based simultaneous multiview imaging greatly improves volumetric imaging speeds, providing sustained image acquisition rates on the order of 175 million voxels per second. This performance exceeds that obtained with state-of-the-art point-scanning imaging techniques by a factor of 10 to 100 and enabled, for example, recording the morphogenesis of entire *Drosophila* embryos at 30-s intervals throughout their development (*25*) (movie S6, study "b" in Fig. 3B). Considering that light-sheet microscopy benefits directly from advances in high-speed camera technology, such as the recent progress in scientific complementary metal oxide semiconductor (sCMOS) technology, a further increase in imaging speed by at least a factor of 10 can be expected in the near future (*16*).

The techniques discussed in this section have been implemented only recently and, for the most part, only proof-of-principle experiments have been performed. Considering the high relevance of their new capabilities for biological live-imaging applications, these methods are likely to quickly find their way into studies of morphogenesis.

Advancing Our Understanding of Morphogenesis with Live Imaging

The use of live-imaging strategies and their combination with optical sample manipulation, computational modeling, and quantitative image analysis are indispensable for advancing our understanding of the key mechanisms driving morphogenesis. Imaging-based investigations enable, for example,

cell lineage tracing in the developing organism (*35*), analyzing the role of signaling pathways in directing morphogenetic events (*36*), and studying the role of physical forces in local and tissue-wide morphogenetic changes (*8*, *37*). The most frequently used model systems in such studies include the fruit fly, zebrafish, and mouse (Fig. 4).

Fruit Fly

Drosophila melanogaster is a well-established model system in developmental biology, owing to the exceptionally wide spectrum of readily available genetic tools. However, resolving cellular dynamics in early development requires imaging approaches with excellent optical penetration (Fig. 5A), because light is strongly scattered and absorbed in the *Drosophila* embryo (*38*).

Live imaging with two-photon fluorescence microscopy is well suited to revealing dynamic processes deep inside the embryo. Using this method, a link between differential positioning of adherens junctions and the initiation of epithelial folding was recently uncovered (*39*) (Fig. 4A and movie S14). These observations (study "d" in Fig. 3B) showed that by modulating epithelial apical-basal polarity, adherens junctions shift basally in those cells that are about to initiate dorsal transverse folds in the early *Drosophila* embryo. This basal shift alters the shape of initiating cells and forces the lateral membrane of adjacent cells to bend toward the initiating cells (*39*).

For imaging superficial tissues, one-photon excitation strategies are advantageous, as they have the potential to yield excellent signal-to-noise ratios at higher image-acquisition speeds. Fast time-lapse imaging of the entire *Drosophila* dorsal thorax with spinning-disk confocal microscopy (study "f" in Fig. 3B), in combination with quantitative image analysis and physical modeling, provided new insights into the control of tissue morphogenesis by signaling pathways (*36*) (Fig. 4B and movie S9). This imaging-based approach revealed how the Fat/Dachsous/Four-Jointed planar cell polarity (PCP) pathway controls morphogenesis of the thorax. It linked the planar polarization established via this pathway to the generation of anisotropy of junction tension by the myosin Dachs and demonstrated that this anisotropy leads to oriented cell rearrangements (*36*).

Zebrafish

Zebrafish embryos and larvae lend themselves particularly well to live-imaging studies using light microscopy, owing to their optical transparency.

A recent multidisciplinary study combining live imaging of zebrafish gastrulation with confocal fluorescence microscopy (Fig. 4C and movies S11 and S12), computational modeling, and optical manipulation through laser ablation (Fig. 4C') revealed the mechanism that allows the contractile actomyosin ring to drive the spreading of the enveloping cell layer over the yolk cell (*37*). Detailed modeling of the forces acting during this morphogenetic process, and time-lapse imaging after local disruption of the actomyosin ring by laser cutting (study "g" in Fig. 3B), showed that this ring functions not only by circumferential contraction but also by a flow-friction mechanism. This investigation thus advanced our understanding of the function of actomyosin rings in epithelial morphogenesis and shed new light on the role of cortical flows in morphogenetic pattern formation (*37*).

A related study in the zebrafish model system investigated cell-cell contact formation of progenitor cells and combined these biophysical measurements with in vitro and in vivo imaging experiments of progenitor cell sorting (*8*). This approach helped to clarify the different roles of cell adhesion and cell cortex tension in driving cell sorting during gastrulation: Cell adhesion is needed to mechanically couple cortices at cell-cell contacts and allows cell cortex tension to control expansion of such contacts (*8*).

Mouse

The study of morphogenesis in mammalian model systems is another field exhibiting rapid progress. The mouse constitutes a leading model system in this respect, owing to its close genetic and physiological similarities to humans and the powerful tools available for manipulating its genome. However, preparation and ex utero culturing of mouse embryos for live imaging with light microscopy are challenging, and sophisticated imaging assays are required for light-based analysis of this exceptionally light-sensitive organism (*40*) (movies S13 and S15). Consequently, many basic questions about the developmental dynamics underlying mouse embryogenesis are currently unanswered (*41*). When do morphogen gradients form and start to act on cells? How do the germ layers form on the cellular level? Are the tissue boundaries evident in late stages already established in the pool of early precursor cells?

Whole-embryo live-imaging assays have a high potential to shed new light on mammalian morphogenesis. For example, a recent study examined the role of rosettes—groups of five or

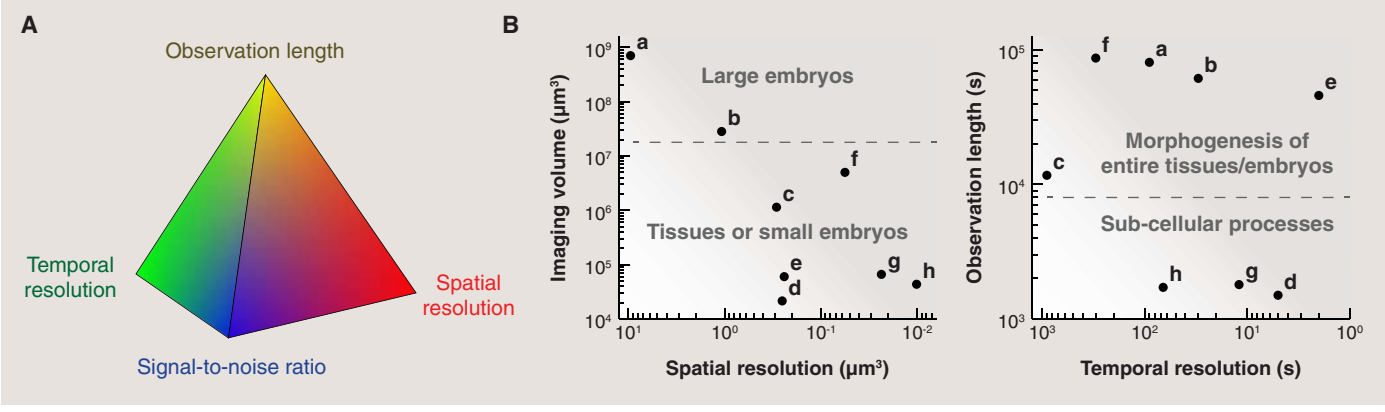

Fig. 3. Parameter space in light-based live imaging of biological specimens. (**A**) The design of in vivo imaging experiments is fundamentally constrained by the light-induced damage capacity of the biological system (maximum allowed amount of light exposure before impacting the biological process) and, for fluorescence microscopy, the total photon yield of the fluorescent markers in the specimen. Many imaging parameters, of which the four most important ones are shown as the corners of the tetrahedron, compete for these two resources and need to be carefully balanced to obtain optimal results in a given experiment. Increasing one parameter intrinsically reduces the maximum performance achievable for at least one of the other parameters. (**B**) Examples of specimen size, spatial resolution (provided as theoretical size of focal volume), observation length, and temporal resolution from eight imaging studies of morphogenetic processes: cell dynamics in entire embryos [a, (*2*); b, (*25*); e, (*3*)], anterior visceral endoderm migration [c, (*42*)], dynamics of adherens junctions [d, (*39*)], morphogenesis of pupal thorax [f, (*36*)], actomyosin flows in the yolk syncytial layer [g, (*37*)], and membrane dynamics in early embryos [h, (*22*)]. These examples involve different model systems [zebrafish (a,g), fruit fly (b,d,f), mouse (c), nematode (e,h)] and imaging techniques [DSLM (a), SiMView (b), confocal (c), two-photon (d), iSPIM (e), spinning disk (f,g), Bessel SR-SIM (h)].

more cells that share a common central vertex—during migration of the anterior visceral endoderm (Fig. 4D and movie S15) (*42*). The visceral endoderm in the egg-cylinder–stage mouse embryo is a continuous epithelial sheet consisting of two regions with very different cellular behaviors: One exhibits cell movement and intercalation, whereas the other is essentially static. By using time-lapse imaging with confocal microscopy (study "c" in Fig. 3B) and computational modeling, rosettes were found to facilitate ordered migration of the anterior visceral endoderm cells within the dynamic region of the epithelium. Interestingly, the rosettes are not formed passively but rather as a result of PCP signaling and buffer the

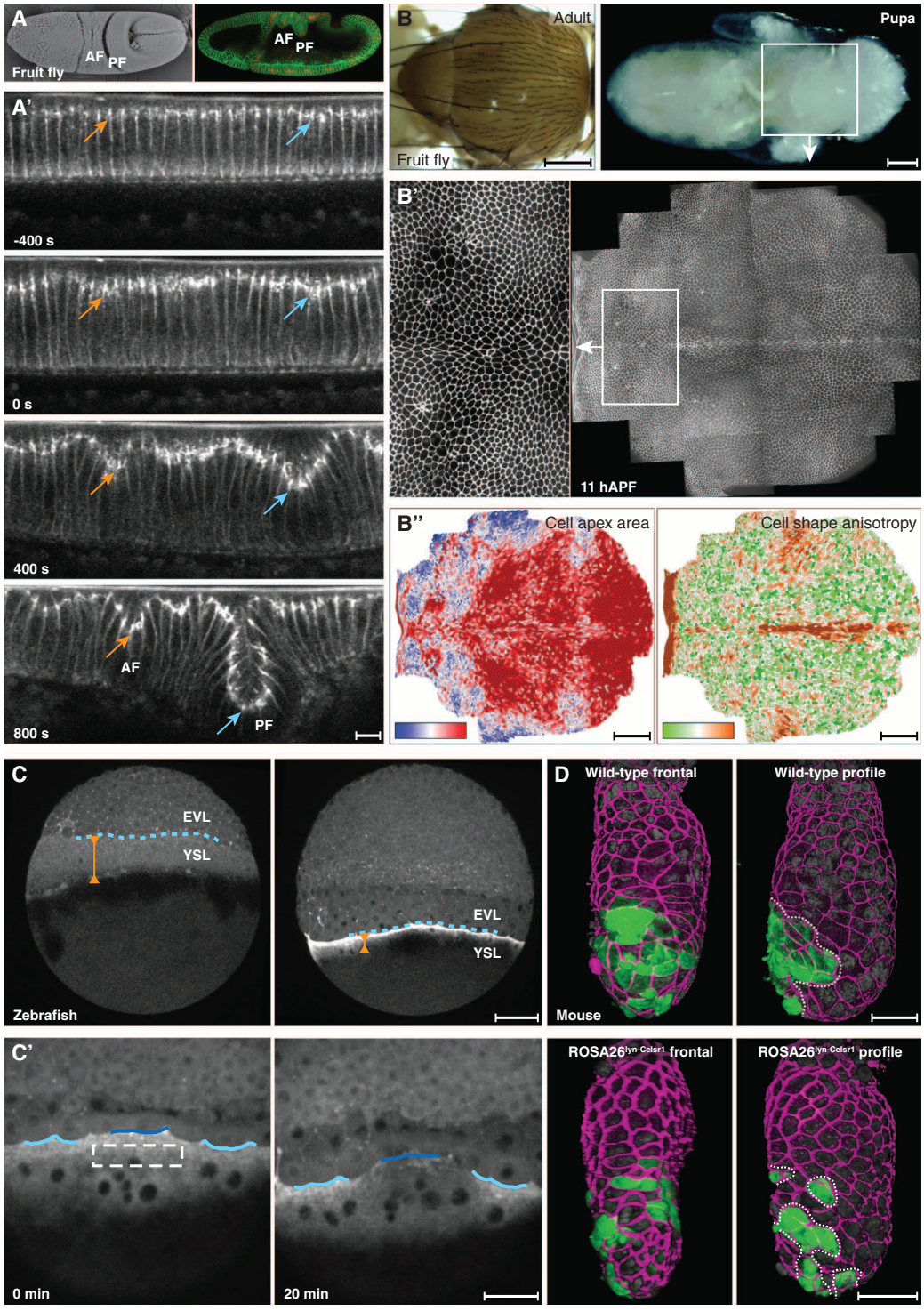

Fig. 4. Advancing our understanding of morphogenesis with live imaging. (**A**) Morphology and cellular dynamics during *Drosophila* dorsal fold formation. Left: Scanning electron micrographs of the dorsal surface in a late *Drosophila* gastrula. Right: Confocal mid-sagittal sections of Neurotactin (green) and Runt (red) immunofluorescence. (A′) Two-photon time-lapse mid-sagittal section of E-Cad:GFP (green fluorescent protein). Arrows, junctions of initiating cells in the anterior (AF, orange) and posterior (PF, cyan) folds undergo basal shift. See movie S14. [Reprinted from (*39*)] (**B**) *Drosophila* dorsal thorax in adult (left) and pupa [right, 11 hours after pupa formation (hAPF), without pupal case]. White box indicates position of thorax. (B′) *Drosophila* pupa dorsal thorax tissue expressing E-Cad:GFP to label apical cell junctions, imaged by multiposition confocal microscopy (24 positions at 5-min resolution). The scutellum is magnified at the left (boxed region). (B″) Cell-level measurements at 11 hAPF. Colors: cell apex area, blue (10 μm^2) to red (60 μm^2); cell shape anisotropy, green (0.1) to brown (0.6). See movie S9. [Reprinted from (*36*)] (**C**) Actomyosin ring morphogenesis and function in zebrafish. In *Tg(actb1:myl12.1-eGFP)* embryos at 40% epiboly (left), an initially diffuse and broad actomyosin band (orange bar) narrows along the animal-vegetal axis to form a distinct cable-like structure at 70% epiboly (right). (C′) Local disruption of the actomyosin ring in *Tg(actb1:myl12.1-eGFP)* embryos at 60% epiboly by consecutive ultraviolet-laser ablation (white dashed rectangle, left) reduces advancement of the adjacent EVL margin (dark blue, right). EVL, enveloping cell layer; YSL, yolk syncytial layer. See movies S11 and S12. [Reprinted from (*37*)] (**D**) Abnormal migration of anterior visceral endoderm (AVE, marked with dotted line in panels to the right) and cellular geometry in mouse mutants with disrupted PCP signaling. Top: En face and profile view of a representative wild-type embryo, illustrating stereotypical ordered migration of AVE cells. Bottom: En face and profile views of an equivalent stage *ROSA26$^{Lyn\text{-}Celsr1}$* mutant, showing abnormal AVE migration. AVE cells appear to have broken into several groups and are spread much more broadly. Magenta: cell outlines (staining for ZO-1); green: AVE cells (Hex-GFP), gray: nuclei (DAPI, 4′,6-diamidino-2-phenylindole). See movie S15. [Reprinted from (*42*)] Scale bars: 250 μm (B), 100 μm (B″, C), 50 μm (C′, D), 10 μm (A′).

disequilibrium in cell packing generated by movement of cells in only one part of the epithelium (*42*).

With the demonstrations of system-level imaging of morphogenesis in fruit fly (*24*–*26*) and zebrafish (*2*), the combination of powerful mammalian embryo culture systems with emerging in vivo imaging technologies will open the door to similar approaches also for mammalian model systems.

Computational Image Analysis and Modeling of Morphogenesis: The Next Frontier

The emergence of powerful live-imaging techniques has turned the generation of large information-rich image data sets of complex biological processes

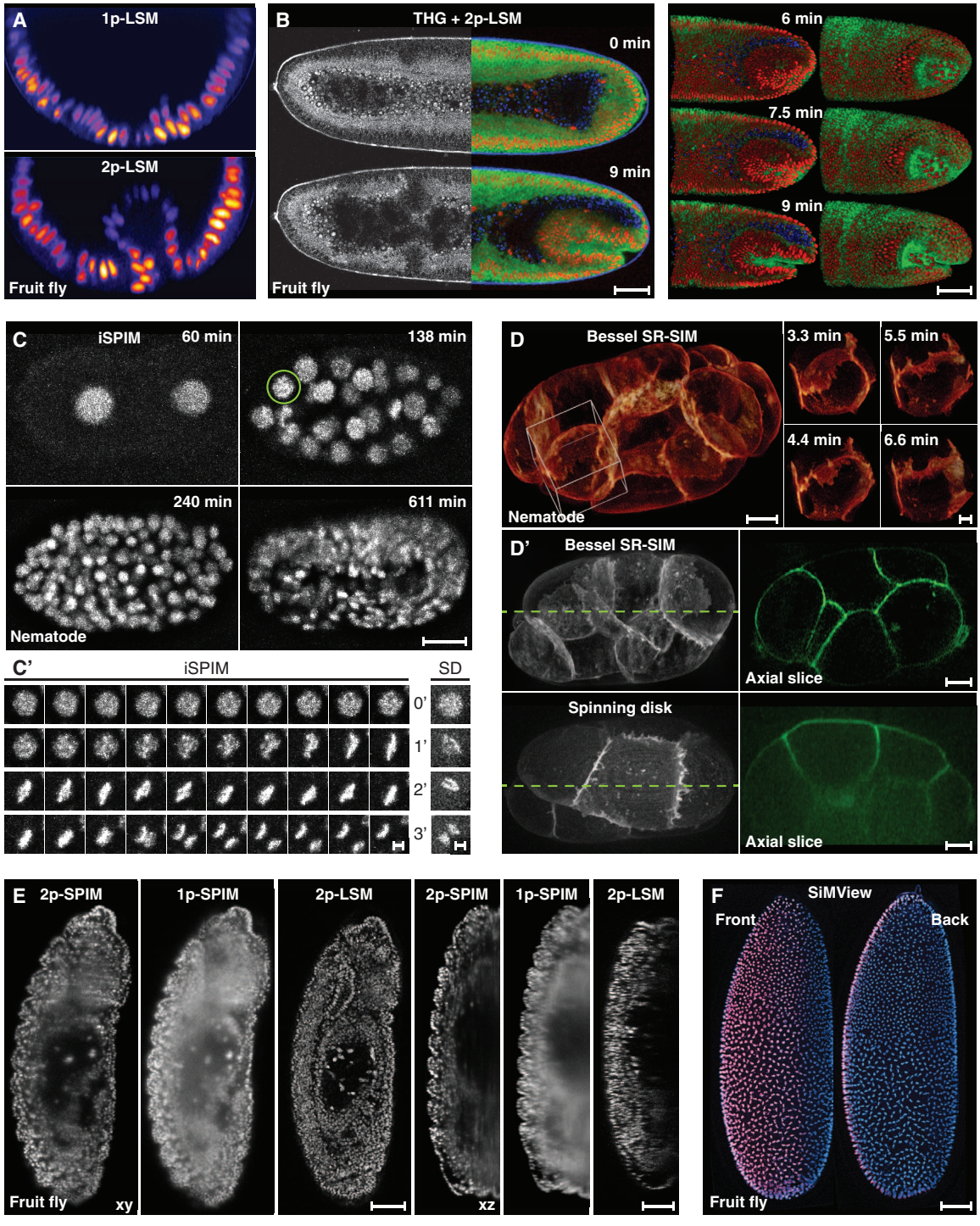

Fig. 5. Emerging imaging techniques for the study of morphogenesis. (**A**) In contrast to one-photon laser-scanning confocal microscopy (1p-LSM, top), two-photon laser-scanning microscopy (2p-LSM, bottom) captures internalized mesoderm cells in histone-GFP–expressing *Drosophila* embryos. See movie S1. [Reprinted from (*1*)] (**B**) Simultaneous multicolor two-photon [2p-LSM, blue: endogenous fluorescence, green: GFP, red: RFP (red fluorescent protein)] and third-harmonic generation (THG) imaging of a developing *Drosophila* embryo. Panels to the right show inner (left) and outer (right) views of the posterior pole region. [Reprinted from (*20*)] (**C**) High-speed inverted selective plane illumination microscopy (iSPIM) imaging (30 volumes/min) of a nuclei-labeled *C. elegans* embryo. (C′) Comparison of iSPIM (sampled every 2 s, shown every 6 s) and spinning disk (SD) confocal microscopy (sampled every 60 s) images. See movies S7 and S8. [Reprinted from (*3*)] (**D**) Bessel plane SR-SIM high-resolution imaging of a membrane-labeled *C. elegans* embryo. Box in top left panel highlights region shown to the right. (D′) In contrast to Bessel plane SR-SIM, spinning disk confocal microscopy images show rapid loss of signal and resolution at depth. See movie S10. [Reprinted from (*22*)] (**E**) Comparison of two-photon light-sheet microscopy (2p-SPIM), one-photon light-sheet microscopy (1p-SPIM) and two-photon laser-scanning microscopy (2p-LSM) images of nuclei-labeled *Drosophila* embryos (left/right: lateral/axial slices). See movie S4. [Reprinted from (*24*)] (**F**) SiMView of an entire nuclei-labeled *Drosophila* embryo. In contrast to single-view light-sheet microscopy, which captures only ~30% of the embryo (red), SiMView provides full physical coverage (blue). See movies S5 and S6. [Reprinted from (*25*)] Scale bars: 50 μm (B, E, F), 10 μm (C), 5 μm (D, left; D′), 2 μm (C′; D, right).

into a routine task. Advanced light-sheet microscopes can record dozens of terabytes of data and millions of high-resolution images per day (*25*). The size of a single whole-embryo imaging experiment obtained with this methodology is comparable to that of the entire book collection of the U.S. Library of Congress. The sheer volume of these recordings thus demands automated approaches of computational image analysis to convert the raw image data into biologically meaningful representations.

However, the tasks needed to extract quantitative information about cell morphology and cell behavior from such data are usually complex and technically challenging. Typical requirements include 3D cell shape segmentation (*43*), accurate cell tracking over time and through cell divisions (*25*, *44*), quantification of expression levels of genes of interest (*5*, *45*), and subcellular localization of proteins (*39*). For example, to quantitatively follow the formation and arrangement of the tens of thousands of cells in a one-day-old zebrafish or fruit fly embryo (Fig. 1B), ~100 million cell positions need to be determined from several thousand volumetric whole-embryo image stacks (movie S16, study "a" in Fig. 3B), considering that a temporal sampling of at most 30 to 60 s is needed to keep up with the speed of cell movements (*2*, *25*). Even when focusing only on morphogenetic processes in a single tissue, the computational challenges are still immense. Speed and scalability of computational methods have thus become as important as their accuracy and robustness.

This first layer of image analysis typically marks only the beginning of the postexperiment analysis. Powerful visualization tools (*46*, *47*) and physical modeling (*48*) are subsequently needed to interpret the resulting data and test mechanistic hypotheses. To reach a system-level understanding of morphogenesis and its multiscale character, the transition from qualitative to quantitative analyses of the underlying biological processes is of key importance. Thus, to keep up with fundamental advances in imaging capabilities, it is now equally important to conceive of new concepts and powerful computational methods to mine the resulting high-content data sets. With the availability of system-level data on cell behavior, gene expression, and likely soon also biophysical tissue properties, we are reaching the point at which it will be feasible to develop computational approaches that incorporate these data into a single model capable of dissecting morphogenesis on the whole-organism level (*15*).

Future Directions

The nature of key breakthroughs in developmental biology in recent years demonstrates that further advancing our understanding of morphogenesis is intrinsically linked to advances in live-imaging technology, development of new approaches to computational data analysis, and seamless integration of physical modeling. It has finally become possible to image entire vertebrate and higher invertebrate embryos throughout their development at a spatiotemporal resolution that enables comprehensive cell tracking, systematic analysis of cell fate determination, reconstruction of single-cell to whole-tissue morphologies, and systematic dissection of the role of physical forces in shaping the developmental building plan.

In coming years, further advances in microscopy technology are expected with high relevance to a wide spectrum of applications in the study of morphogenesis. Ongoing efforts are aimed at advancing deep-tissue in vivo imaging, improving spatial resolution, and increasing temporal sampling. These capabilities will open up exciting new possibilities. For example, resolving the fine spatiotemporal dynamics of subcellular processes on the whole-tissue level will help to elucidate the molecular mechanisms underlying tissue morphogenesis. High-speed volumetric imaging will give access to both development and function of complex biological systems at the same time, from individual tissues and organs, such as the developing heart (*17*), to entire organ systems, such as the nervous system (*16*). Existing assays in light-sheet microscopy already reveal cell behavior on the whole-embryo level, but further improvements, in particular with respect to imaging speed, will make it possible to also systematically measure functional properties of developing tissues, and thus, to determine the reciprocal effect on development.

Combining advanced imaging methods with powerful computational tools will enable not only system-level analyses of morphogenesis but also entirely new experimental approaches. Real-time cell segmentation and cell lineage reconstructions during live imaging of embryonic development could guide functional interference—for example, by using cell positions and computationally predicted cell identities for targeted optical manipulation with laser ablation or optogenetics. Such approaches could be used for the systematic dissection of functional relationships in the developmental building plan on the whole-embryo level.

Imaging-based studies of morphogenesis will also greatly benefit from the development of new fluorescent probes and sensors, including highly photostable and bright infrared fluorescent proteins for deep-tissue imaging, novel fluorescent timer proteins for visualizing signaling and other processes based on protein age and turnover (*4*), and genetically encoded sensors for the quantitative in vivo measurement of physical forces (*49*).

Combining the experimental capabilities and theoretical approaches of these different disciplines will be an indispensable step toward the establishment of a quantitative model of the developing embryo and, thus, a system-level understanding of morphogenesis.

References and Notes

1. A. McMahon, W. Supatto, S. E. Fraser, A. Stathopoulos, Dynamic analyses of *Drosophila* gastrulation provide insights into collective cell migration. *Science* **322**, 1546–1550 (2008). doi: 10.1126/science.1167094; pmid: 19056986
2. P. J. Keller, A. D. Schmidt, J. Wittbrodt, E. H. K. Stelzer, Reconstruction of zebrafish early embryonic development by scanned light sheet microscopy. *Science* **322**, 1065–1069 (2008). doi: 10.1126/science.1162493; pmid: 18845710
3. Y. Wu, A. Ghitani, R. Christensen, A. Santella, Z. Du, G. Rondeau, Z. Bao, D. Colón-Ramos, H. Shroff, Inverted selective plane illumination microscopy (iSPIM) enables coupled cell identity lineaging and neurodevelopmental imaging in *Caenorhabditis elegans*. *Proc. Natl. Acad. Sci. U.S.A.* **108**, 17708–17713 (2011). doi: 10.1073/pnas.1108494108; pmid: 22006307
4. A. Khmelinskii, P. J. Keller, A. Bartosik, M. Meurer, J. D. Barry, B. R. Mardin, A. Kaufmann, S. Trautmann, M. Wachsmuth, G. Pereira, W. Huber, E. Schiebel, M. Knop, Tandem fluorescent protein timers for in vivo analysis of protein dynamics. *Nat. Biotechnol.* **30**, 708–714 (2012). doi: 10.1038/nbt.2281; pmid: 22729030
5. C. C. Fowlkes, C. L. Hendriks, S. V. Keränen, G. H. Weber, O. Rübel, M. Y. Huang, S. Chatoor, A. H. DePace, L. Simirenko, C. Henriquez, A. Beaton, R. Weiszmann, S. Celniker, B. Hamann, D. W. Knowles, M. D. Biggin, M. B. Eisen, J. Malik, A quantitative spatiotemporal atlas of gene expression in the *Drosophila* blastoderm. *Cell* **133**, 364–374 (2008). doi: 10.1016/j.cell.2008.01.053; pmid: 18423206
6. B. Wu, K. D. Piatkevich, T. Lionnet, R. H. Singer, V. V. Verkhusha, Modern fluorescent proteins and imaging technologies to study gene expression, nuclear localization, and dynamics. *Curr. Opin. Cell Biol.* **23**, 310–317 (2011). doi: 10.1016/j.ceb.2010.12.004; pmid: 21242078
7. G. T. Reeves, N. Trisnadi, T. V. Truong, M. Nahmad, S. Katz, A. Stathopoulos, Dorsal-ventral gene expression in the *Drosophila* embryo reflects the dynamics and precision of the dorsal nuclear gradient. *Dev. Cell* **22**, 544–557 (2012). doi: 10.1016/j.devcel.2011.12.007; pmid: 22342544
8. J. L. Maître, H. Berthoumieux, S. F. Krens, G. Salbreux, F. Jülicher, E. Paluch, C. P. Heisenberg, Adhesion functions in cell sorting by mechanically coupling the cortices of adhering cells. *Science* **338**, 253–256 (2012). doi: 10.1126/science.1225399; pmid: 22923438
9. C. Guillot, T. Lecuit, Mechanics of epithelial tissue homeostasis and morphogenesis. *Science* **340**, 1185 (2013).
10. W. Denk, J. H. Strickler, W. W. Webb, Two-photon laser scanning fluorescence microscopy. *Science* **248**, 73–76 (1990). doi: 10.1126/science.2321027; pmid: 2321027
11. A. H. Voie, D. H. Burns, F. A. Spelman, Orthogonal-plane fluorescence optical sectioning: Three-dimensional imaging of macroscopic biological specimens. *J. Microsc.* **170**, 229–236 (1993). doi: 10.1111/j.1365-2818.1993.tb03346.x; pmid: 8371260
12. J. Huisken, J. Swoger, F. Del Bene, J. Wittbrodt, E. H. K. Stelzer, Optical sectioning deep inside live embryos by selective plane illumination microscopy. *Science* **305**, 1007–1009 (2004). doi: 10.1126/science.1100035; pmid: 15310904
13. H. Siedentopf, R. Zsigmondy, Über Sichtbarmachung und Größenbestimmung ultramikroskopischer Teilchen, mit besonderer Anwendung auf Goldrubingläser. *Annalen der Physik* **315**, 1–39 (1902). doi: 10.1002/andp.19023150102
14. J. Mertz, Optical sectioning microscopy with planar or structured illumination. *Nat. Methods* **8**, 811–819 (2011). doi: 10.1038/nmeth.1709; pmid: 21959136
15. K. Khairy, P. J. Keller, Reconstructing embryonic development. *Genesis* **49**, 488–513 (2011). doi: 10.1002/dvg.20698; pmid: 21140407

16. M. B. Ahrens, M. B. Orger, D. N. Robson, J. M. Li, P. J. Keller, Whole-brain functional imaging at cellular resolution using light-sheet microscopy. *Nat. Methods* **10**, 413–420 (2013). doi: 10.1038/nmeth.2434; pmid: 23524393
17. A. B. Arrenberg, D. Y. Stainier, H. Baier, J. Huisken, Optogenetic control of cardiac function. *Science* **330**, 971–974 (2010). doi: 10.1126/science.1195929; pmid: 21071670
18. N. Ji, D. E. Milkie, E. Betzig, Adaptive optics via pupil segmentation for high-resolution imaging in biological tissues. *Nat. Methods* **7**, 141–147 (2010). doi: 10.1038/nmeth.1411; pmid: 20037592
19. K. Si, R. Fiolka, M. Cui, Fluorescence imaging beyond the ballistic regime by ultrasound pulse guided digital phase conjugation. *Nat. Photonics* **6**, 657–661 (2012). doi: 10.1038/nphoton.2012.205; pmid: 23241552
20. P. Mahou, M. Zimmerley, K. Loulier, K. S. Matho, G. Labroille, X. Morin, W. Supatto, J. Livet, D. Débarre, E. Beaurepaire, Multicolor two-photon tissue imaging by wavelength mixing. *Nat. Methods* **9**, 815–818 (2012). doi: 10.1038/nmeth.2098; pmid: 22772730
21. T. A. Planchon, L. Gao, D. E. Milkie, M. W. Davidson, J. A. Galbraith, C. G. Galbraith, E. Betzig, Rapid three-dimensional isotropic imaging of living cells using Bessel beam plane illumination. *Nat. Methods* **8**, 417–423 (2011). doi: 10.1038/nmeth.1586; pmid: 21378978
22. L. Gao, L. Shao, C. D. Higgins, J. S. Poulton, M. Peifer, M. W. Davidson, X. Wu, B. Goldstein, E. Betzig, Noninvasive imaging beyond the diffraction limit of 3D dynamics in thickly fluorescent specimens. *Cell* **151**, 1370–1385 (2012). doi: 10.1016/j.cell.2012.10.008; pmid: 23217717
23. J. Capoulade, M. Wachsmuth, L. Hufnagel, M. Knop, Quantitative fluorescence imaging of protein diffusion and interaction in living cells. *Nat. Biotechnol.* **29**, 835–839 (2011). doi: 10.1038/nbt.1928; pmid: 21822256
24. T. V. Truong, W. Supatto, D. S. Koos, J. M. Choi, S. E. Fraser, Deep and fast live imaging with two-photon scanned light-sheet microscopy. *Nat. Methods* **8**, 757–760 (2011). doi: 10.1038/nmeth.1652; pmid: 21765409
25. R. Tomer, K. Khairy, F. Amat, P. J. Keller, Quantitative high-speed imaging of entire developing embryos with simultaneous multiview light-sheet microscopy. *Nat. Methods* **9**, 755–763 (2012). doi: 10.1038/nmeth.2062; pmid: 22660741
26. U. Krzic, S. Gunther, T. E. Saunders, S. J. Streichan, L. Hufnagel, Multiview light-sheet microscope for rapid in toto imaging. *Nat. Methods* **9**, 730–733 (2012). doi: 10.1038/nmeth.2064; pmid: 22660739
27. F. O. Fahrbach, P. Simon, A. Rohrbach, Microscopy with self-reconstructing beams. *Nat. Photonics* **4**, 780–785 (2010). doi: 10.1038/nphoton.2010.204
28. M. A. Neil, R. Juskaitis, T. Wilson, Method of obtaining optical sectioning by using structured light in a conventional microscope. *Opt. Lett.* **22**, 1905–1907 (1997). doi: 10.1364/OL.22.001905; pmid: 18188403
29. M. G. Gustafsson, L. Shao, P. M. Carlton, C. J. Wang, I. N. Golubovskaya, W. Z. Cande, D. A. Agard, J. W. Sedat, Three-dimensional resolution doubling in wide-field fluorescence microscopy by structured illumination. *Biophys. J.* **94**, 4957–4970 (2008). doi: 10.1529/biophysj.107.120345; pmid: 18326650
30. P. J. Keller, A. D. Schmidt, A. Santella, K. Khairy, Z. Bao, J. Wittbrodt, E. H. Stelzer, Fast, high-contrast imaging of animal development with scanned light sheet-based structured-illumination microscopy. *Nat. Methods* **7**, 637–642 (2010). doi: 10.1038/nmeth.1476; pmid: 20601950
31. M. J. Booth, Adaptive optics in microscopy. *Philos. Trans R Soc A* **365**, 2829–2843 (2007). doi: 10.1098/rsta.2007.0013; pmid: 17855218
32. X. Xu, H. Liu, L. V. Wang, Time-reversed ultrasonically encoded optical focusing into scattering media. *Nat. Photonics* **5**, 154–157 (2011). doi: 10.1038/nphoton.2010.306; pmid: 21532925
33. N. C. Shaner, R. E. Campbell, P. A. Steinbach, B. N. Giepmans, A. E. Palmer, R. Y. Tsien, Improved monomeric red, orange and yellow fluorescent proteins derived from *Discosoma* sp. red fluorescent protein. *Nat. Biotechnol.* **22**, 1567–1572 (2004). doi: 10.1038/nbt1037; pmid: 15558047
34. D. M. Chudakov, M. V. Matz, S. Lukyanov, K. A. Lukyanov, Fluorescent proteins and their applications in imaging living cells and tissues. *Physiol. Rev.* **90**, 1103–1163 (2010). doi: 10.1152/physrev.00038.2009; pmid: 20664080
35. P. B. Abitua, E. Wagner, I. A. Navarrete, M. Levine, Identification of a rudimentary neural crest in a non-vertebrate chordate. *Nature* **492**, 104–107 (2012). doi: 10.1038/nature11589; pmid: 23135395
36. F. Bosveld, I. Bonnet, B. Guirao, S. Tlili, Z. Wang, A. Petitalot, R. Marchand, P. L. Bardet, P. Marcq, F. Graner, Y. Bellaïche, Mechanical control of morphogenesis by Fat/Dachsous/Four-jointed planar cell polarity pathway. *Science* **336**, 724–727 (2012). doi: 10.1126/science.1221071; pmid: 22499807
37. M. Behrndt, G. Salbreux, P. Campinho, R. Hauschild, F. Oswald, J. Roensch, S. W. Grill, C. P. Heisenberg, Forces driving epithelial spreading in zebrafish gastrulation. *Science* **338**, 257–260 (2012). doi: 10.1126/science.1224143; pmid: 23066079
38. W. Supatto, A. McMahon, S. E. Fraser, A. Stathopoulos, Quantitative imaging of collective cell migration during *Drosophila* gastrulation: Multiphoton microscopy and computational analysis. *Nat. Protoc.* **4**, 1397–1412 (2009). doi: 10.1038/nprot.2009.130; pmid: 19745822
39. Y. C. Wang, Z. Khan, M. Kaschube, E. F. Wieschaus, Differential positioning of adherens junctions is associated with initiation of epithelial folding. *Nature* **484**, 390–393 (2012). doi: 10.1038/nature10938; pmid: 22456706
40. A. Piliszek, G. S. Kwon, A. K. Hadjantonakis, Ex utero culture and live imaging of mouse embryos. *Methods Mol. Biol.* **770**, 243–257 (2011). doi: 10.1007/978-1-61779-210-6_9; pmid: 21805267
41. S. Nowotschin, A. K. Hadjantonakis, Cellular dynamics in the early mouse embryo: From axis formation to gastrulation. *Curr. Opin. Genet. Dev.* **20**, 420–427 (2010). doi: 10.1016/j.gde.2010.05.008; pmid: 20566281
42. G. Trichas, A. M. Smith, N. White, V. Wilkins, T. Watanabe, A. Moore, B. Joyce, J. Sugnaseelan, T. A. Rodriguez, D. Kay, R. E. Baker, P. K. Maini, S. Srinivas, Multi-cellular rosettes in the mouse visceral endoderm facilitate the ordered migration of anterior visceral endoderm cells. *PLoS Biol.* **10**, e1001256 (2012). doi: 10.1371/journal.pbio.1001256; pmid: 22346733
43. R. Fernandez, P. Das, V. Mirabet, E. Moscardi, J. Traas, J. L. Verdeil, G. Malandain, C. Godin, Imaging plant growth in 4D: Robust tissue reconstruction and lineaging at cell resolution. *Nat. Methods* **7**, 547–553 (2010). doi: 10.1038/nmeth.1472; pmid: 20543845
44. Z. Bao, J. I. Murray, T. Boyle, S. L. Ooi, M. J. Sandel, R. H. Waterston, Automated cell lineage tracing in *Caenorhabditis elegans*. *Proc. Natl. Acad. Sci. U.S.A.* **103**, 2707–2712 (2006). doi: 10.1073/pnas.0511111103; pmid: 16477039
45. J. I. Murray, Z. Bao, T. J. Boyle, M. E. Boeck, B. L. Mericle, T. J. Nicholas, Z. Zhao, M. J. Sandel, R. H. Waterston, Automated analysis of embryonic gene expression with cellular resolution in *C. elegans*. *Nat. Methods* **5**, 703–709 (2008). doi: 10.1038/nmeth.1228; pmid: 18587405
46. H. Peng, Z. Ruan, F. Long, J. H. Simpson, E. W. Myers, V3D enables real-time 3D visualization and quantitative analysis of large-scale biological image data sets. *Nat. Biotechnol.* **28**, 348–353 (2010). doi: 10.1038/nbt.1612; pmid: 20231818
47. K. W. Eliceiri, M. R. Berthold, I. G. Goldberg, L. Ibáñez, B. S. Manjunath, M. E. Martone, R. F. Murphy, H. Peng, A. L. Plant, B. Roysam, N. Stuurman, J. R. Swedlow, P. Tomancak, A. E. Carpenter, Biological imaging software tools. *Nat. Methods* **9**, 697–710 (2012). doi: 10.1038/nmeth.2084; pmid: 22743775
48. A. C. Oates, N. Gorfinkiel, M. González-Gaitán, C. P. Heisenberg, Quantitative approaches in developmental biology. *Nat. Rev. Genet.* **10**, 517–530 (2009). doi: 10.1038/nrg2548; pmid: 19584811
49. C. Grashoff, B. D. Hoffman, M. D. Brenner, R. Zhou, M. Parsons, M. T. Yang, M. A. McLean, S. G. Sligar, C. S. Chen, T. Ha, M. A. Schwartz, Measuring mechanical tension across vinculin reveals regulation of focal adhesion dynamics. *Nature* **466**, 263–266 (2010). doi: 10.1038/nature09198; pmid: 20613844

Acknowledgments: I thank K. Branson for helpful discussions and help with preparing the figures; Y. Wan and W. Lemon for help with recording the zebrafish SiMView data set; and F. Amat, Y. Bellaïche, E. Betzig, M. Handberg-Thorsager, B. Hoeckendorf, K. Khairy, M. Knop, W. Lemon, J. Liu, K. McDole, S. Srinivas, D. Stern and Y. Wan for helpful comments on the manuscript. This work was supported by the Howard Hughes Medical Institute.

Supplementary Materials

www.sciencemag.org/content/340/6137/1234168/suppl/DC1
References (*50*, *51*)
Movies S1 to S16

10.1126/science.1234168

REVIEW SUMMARY

Imaging Morphogenesis: Technological Advances and Biological Insights

Philipp J. Keller

READ THE FULL ARTICLE ONLINE
http://dx.doi.org/10.1126/science.1234168

Cite this article as P. J. Keller, *Science* **340**, 1234168 (2013). DOI: 10.1126/science.1234168

Background: Our understanding of developmental processes relies fundamentally on their in vivo observation. Morphogenesis, the shaping of an organism by cell movements, cell-cell interactions, collective cell behavior, cell shape changes, cell divisions, and cell death, is a dynamic process on many scales, from fast subcellular rearrangements to slow structural changes at the whole-organism level. The ability to capture, simultaneously, the fast dynamic behavior of individual cells, as well as their system-level interactions over long periods of time, is crucial for an understanding of the underlying biological mechanisms. Arriving at a complete picture of morphogenesis requires not only observation of single-cell to tissue-level morphological dynamics, but also quantitative measurement of protein dynamics, changes in gene expression, and readouts of physical forces acting during development. Live-imaging approaches based on light microscopy are of key importance to obtaining such information at the system level and with high spatiotemporal resolution.

Advances: Live imaging with light microscopy requires carefully balancing competing parameters, among which spatiotemporal resolution and light exposure of the living specimen are chief. To maximize the quantity and quality of information extracted from the specimen under observation, optimal use must be made of the limited number of photons that can be collected under physiological conditions. Emerging techniques for noninvasive in vivo imaging can record morphogenetic processes at temporal scales from seconds to days and at spatial scales from hundreds of nanometers to several millimeters, with minimal energy load on the specimen. These approaches are able to capture cellular dynamics in entire vertebrate and higher invertebrate embryos throughout their development. It has become possible to follow cell movements, cell shape dynamics, subcellular protein localization, and changes in gene expression simultaneously, for the entire undisturbed living system. The application of these methods to the study of morphogenesis in the fly, fish, and mouse has led to fundamental insights into the mechanisms underlying epithelial folding, the control of tissue morphogenesis by signaling pathways, and the role of physical forces in local and tissue-wide morphogenetic changes.

Outlook: Current efforts in microscopy technology development are aimed at advancing deep-tissue in vivo imaging, improving spatial resolution, and increasing temporal sampling. To unlock their full potential, these methods need to be matched with new computational approaches and physical models that help convert the resulting, highly complex image data sets into biological insights. With the availability of system-level data on cell behavior and gene expression, and the potential for a system-level analysis of biophysical tissue properties, we are reaching the point at which it will be feasible to develop computational approaches that incorporate these data into a single model capable of dissecting morphogenesis at the whole-organism level.

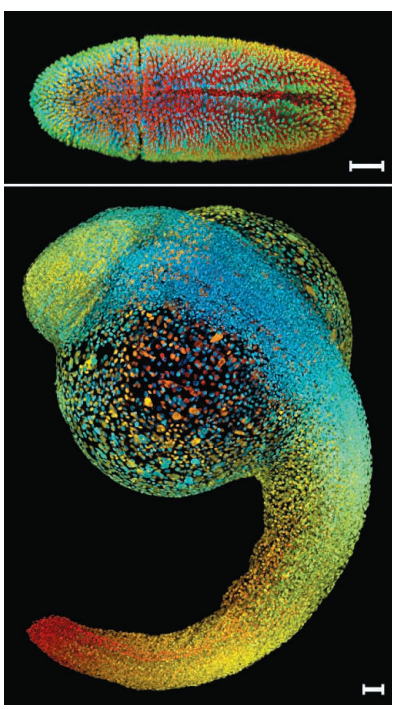

Live imaging of embryonic development. Nuclei-labeled *Drosophila* (**top**) and zebrafish (**bottom**) embryos were imaged with a simultaneous multiview light-sheet microscope (SiMView). The embryos are shown at 3 and 22 hours postfertilization, respectively. Color indicates depth in the image. Scale bars: 50 μm.

Howard Hughes Medical Institute, Janelia Farm Research Campus, 19700 Helix Drive, Ashburn, VA 20147, USA.
E-mail: kellerp@janelia.hhmi.org

ARTICLE OUTLINE

BACKGROUND READING

J. Mertz, Optical sectioning microscopy with planar or structured illumination. *Nat. Methods* **8**, 811 (2011). doi:10.1038/nmeth.1709

A. C. Oates, N. Gorfinkiel, M. González-Gaitán, C. P. Heisenberg, Quantitative approaches in developmental biology. *Nat. Rev. Genet.* **10**, 517 (2009). doi:10.1038/nrg2548

S. G. Megason, S. E. Fraser, Imaging in systems biology. *Cell* **130**, 784 (2007). doi:10.1016/j.cell.2007.08.031

K. Khairy, P. J. Keller, Reconstructing embryonic development. *Genesis* **49**, 488 (2011). doi:10.1002/dvg.20698

M. Behrndt *et al.*, Forces driving epithelial spreading in zebrafish gastrulation. *Science* **338**, 257 (2012). doi:10.1126/science.1224143

F. Bosveld *et al.*, Mechanical control of morphogenesis by Fat/Dachsous/Four-jointed planar cell polarity pathway. *Science* **336**, 724 (2012). doi:10.1126/science.1221071

Y. C. Wang, Z. Khan, M. Kaschube, E. F. Wieschaus, Differential positioning of adherens junctions is associated with initiation of epithelial folding. *Nature* **484**, 390 (2012). doi:10.1038/nature10938